SMHI

No 92, November 2000

Reports Meteorology and Climatology

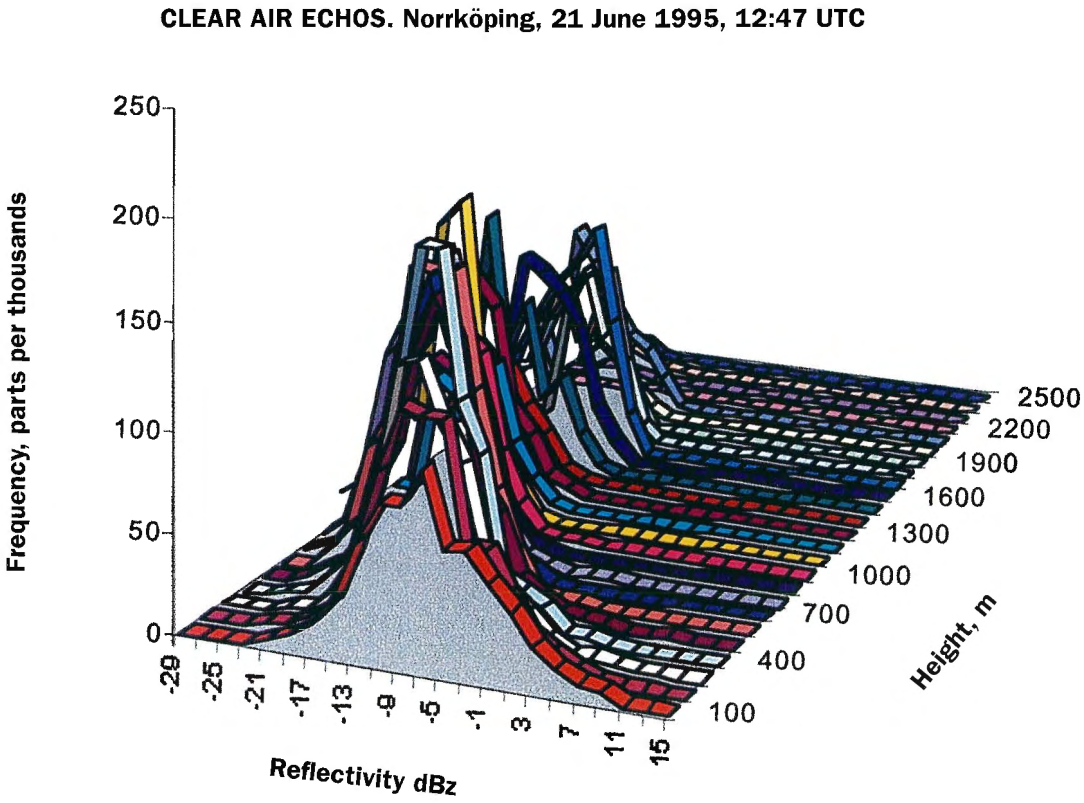

Boundary layer clear air radar echos in southern Sweden

Tage Andersson

Cover: Relative frequency distributions of clear air echos in the atmospheric boundary layer a summer day. The distributions are given for each 100 m height gate.

RMK
No 92, November 2000

Boundary layer clear air radar echos in southern Sweden

Tage Andersson

Report Summary / Rapportsammanfattning

Issuing Agency/Utgivare	Report number/Publikation
Swedish Meteorological and Hydrological Institute S-601 76 NORRKÖPING Sweden	RMK No. 92
	Report date/Utgivningsdatum November 2000

Author (s)/Författare

Tage Andersson

Title (and Subtitle/Titel

Boundary layer clear air radar echos in southern Sweden

Abstract/Sammandrag

The C band weather radars of today are sensitive enough to record clear air echos from the boundary layer during the warmer seasons even in latitudes as high as Scandinavia. Such clear air echos have long been recognised in the US and a. o. used to retrieve the wind. Curiously enough, in Europe there has been, and perhaps still is, a wide spread belief among meteorologists that boundary layer clear air echos are absent there. The probable reason is that since European weather radars are almost only used to monitor precipitation, in most countries weak echos, supposed not to represent precipitation, are suppressed. This may be performed in many ways, for instance by using the STC (Sensitivity Time Control, also called Swept Gain) which suppresses echos close to the radar, or by thresholding weak echos in the radar images used. The threshold is usually about 10 dBz, and since most clear air echos are weaker, they do not appear in the images, though the radar might have recorded them.

That these clear air echos actually are echos from the air, as from sharp refractive index gradients, insects or birds, is evident since Doppler radars show that they move, generally approximately with the winds recorded by other means. The exceptions are from targets heading towards a specific goal, as migrating birds, birds leaving a nocturnal roost and locust swarms.

The concept 'clear air echos' refers to echos from a non-precipitating atmosphere. There is no commonly agreed stringent definition of clear air echos.

Key words/sök-, nyckelord

Weather radar, clear air echos, echos from birds, echos from insects, radar ornithology, radar entomology

Supplementary notes/Tillägg	Number of pages/Antal sidor	Language/Språk
	22	English

ISSN and title/ISSN och titel

0347-2116 SMHI Reports Meteorology Climatology

Report available from/Rapporten kan köpas från:

SMHI
S-601 76 NORRKÖPING
Sweden

1. Introduction

This paper will give some statistics about clear air echos in southern Sweden, as their frequencies, reflectivities and vertical extent. The data are obtained with Ericsson C band Doppler weather radars of the Swedish weather radar network, mainly the Norrköping radar (58 ° N, 16.15 ° E, 58 m above M.S.L.) and the Gothenburg radar (57.72 °N, 12.17 °E, 164 m above MSL). For technical radar data, see the appendix.

Radar echos from 'clear air', that is from non-precipitation air, have been observed since the beginning of radar observations. Their origin, from insects, birds or sharp gradients of the refractivity index of the air, has been debated as long. Already in the late 1930s it was found that certain radars could detect birds. Insects as radar echo sources are known since the 1940s. Although the origin of these echos was debated through the 1960s, around 1970 insects and birds were recognised as the primary source of clear air echos (Vaughn, 1985). Radar has been used by ornithologists for bird studies and by entomologists for insect studies. However, clear air echos at temperatures below 0° C during winter can hardly be explained by insects. Such echos have a. o. been observed by the Norrköping radar. A possible source is sharp gradients in the refractive index of the air (Battan 1973, Wilson 1994).

In 1996 an error of the Ericsson radar was detected. It resulted in 5 dBz too high reflectivities in the non-Doppler mode. Most of the data used here originate from the Doppler mode, and when reference is made to non-Doppler reflectivities, this will be mentioned. The error was corrected in the autumn of 1997.

2. How the reflectivity profiles were obtained

The Doppler mode was used, and ground echos were rejected with a filter excluding echos with radial velocities close to 0 m/s. The range gates have a length of 1 km, and one complete revolution of the antenna contains 420 azimuth gates. The scan scheme underwent only small changes during the experiment, and the elevation angles of the most used one are given in Table 1.

Table 1. Elevation angles of the Doppler mode scan scheme.

No	*1*	*2*	*3*	*4*	*5*	*6*	*7*	*8*	*9*	*10*	*11*	*12*	*13*	*14*	*15*
Deg.	*0.5*	*0.9*	*1.5*	*2.5*	*3.5*	*4.5*	*6.0*	*7.5*	*9.0*	*11.0*	*13.0*	*15.0*	*20.0*	*30.0*	*45.0*

The reflectivities are given with a resolution of 0.4 dBz. A height resolution of 100 m was selected, and for each height gate the following statistics of reflectivity were computed, using data from all elevation and azimuth angles within a radius of 15 km:

- Relative frequencies, in 2 dBz intervals
- Arithmetic mean
- Median value
- Most common value
- Maximum value

When computing the arithmetic mean, the median value and the most common value, pixel values 0, that is no echo, were excluded, as well as all maximum pixel values (255). An example of a part of these computations is given in Table 2.

Table 2. Example of the vertical profile data. The x axis gives height in hectometer, hm, lines 4 and 8. Lines between the height scale (lines 5-7) give average, am, median, mv, and most common , mo, reflectivities. The numbers in the first column below line 8 give the reflectivity factor in dBz, and the other columns give relative frequencies in parts per thousand. -31 is no echo This is only an example. In the routine runs heights up to 50 hectometers and reflectivities to 69 dBz were recorded.

21-JUN-1995 09:47:12 S240R1 QUA_Z Norrkoeping																
HEIGHT RESOLUTION IS 100 M																
FREQS OF dBz FOR 1 TO 31 HECTOM, AZIM 0 TO 358 deg																
hm	1	2	3	4	5	6	7	8	9	10	11	12	13	14	15	16
am	-10	-12	-13	-14	-16	-18	-19	-20	-20	-21	-21	-21	-23	-22	-23	-22
mv	-9	-11	-13	-15	-15	-17	-19	-19	-21	-21	-21	-21	-23	-23	-23	-23
mo	-7	-11	-13	-17	-15	-21	-19	-21	-19	-21	-21	-19	-23	-25	-25	-23
hm	1	2	3	4	5	6	7	8	9	10	11	12	13	14	15	16
-31	434	390	397	309	405	324	502	320	510	508	427	747	515	576	675	677
-29	0	1	4	3	2	3	0	10	18	11	24	0	0	41	23	49
-27	1	2	6	7	3	13	16	17	33	40	55	0	76	24	8	48
-25	5	5	5	17	16	38	29	73	47	83	47	56	57	89	110	35
-23	10	16	32	33	49	64	45	107	85	78	122	49	148	79	59	81
-21	19	33	37	61	55	109	81	115	89	86	124	53	112	82	65	69
-19	25	35	41	73	77	109	106	114	97	78	91	59	59	58	20	28
-17	36	46	37	87	77	106	90	114	60	55	58	27	20	32	25	6
-15	42	52	68	86	87	90	65	76	36	34	33	4	5	9	4	2
-13	56	68	93	87	85	76	39	35	15	17	12	0	3	1	5	0
-11	59	84	78	75	72	34	15	10	3	4	2	0	0	1	0	0
-9	43	57	51	48	29	17	3	2	1	0	0	0	0	0	0	0
-7	60	68	51	53	28	7	2	0	0	1	0	0	0	0	0	0
-5	37	34	35	27	5	0	0	0	0	0	0	0	0	0	0	0
-3	51	49	34	17	2	0	0	0	0	0	0	0	0	0	0	0
-1	44	30	15	6	0	1	0	0	0	0	0	0	0	0	0	0
1	29	13	5	2	0	0	0	0	0	0	0	0	0	0	0	0
3	14	3	1	0	0	0	0	0	0	0	0	0	0	0	0	0
5	8	1	0	0	0	0	0	0	0	0	0	0	0	0	0	0
7	6	0	0	0	0	0	0	0	0	0	0	0	0	0	0	0
9	4	0	0	0	0	0	0	0	0	0	0	0	0	0	0	0
11	2	0	0	0	0	0	0	0	0	0	0	0	0	0	0	0
13	1	0	0	0	0	0	0	0	0	0	0	0	0	0	0	0

3. Examples of clear air echos

Fig 1 shows characteristic patterns of clear air echos from 5 radars (and part of them from another 3 radars) during early summer at midday. Coasts drawn with thin black lines, while thick lines give the borders of radar surveillance areas. The clear air echos are non-structured patches of weak echos, surrounding the radar out to varying radii, generally less than 100 km. The echos mostly occur over land and at their seaward sides they roughly depict the coast. The Karlskrona radar even paints the southern part of the island of Öland with echos, but the strait between the mainland and the island is mostly free from echos. Over the Baltic sea anomal propagation conditions prevailed and the Gotland radar shows anomal (anaprop) echos from coasts as well as from sea waves (sea clutter). The vertical reflectivity structure over the Norrköping radar is given in Fig. 2. The winds derived from these echos are also shown in Fig. 2. The VAD technique of the Swedish Meteorological and Hydrological Institute (Andersson, 1992) was used to derive the winds. (VAD=Velocity Azimuth Display, is a technique to retrieve the actual winds from the radial winds given by a Doppler radar). The weather was cloudy, with Cumulus congestus and Cirrostratus and at Norrköping the geostrophic wind was weak, south-westerly

Late summer clear air echos are shown by Fig. 3. Also in this event there was anomalous propagation over the sea and cost-near radars depict far-away coasts and sea waves. The VAD winds, Fig. 4, from Norrköping show that the echos extend up to at least nearly 2500 m. It was nearly cloud-free, only about 1 octa Cirrus.

Most of the Swedish radars have a free horizon, making them very susceptible to ordinary ground echos as well as anaprop echos. This especially applies to the radars of Karlskrona, Gotland and Stockholm/Arlanda. The coast-near radars of Gotland and Karlskrona often show faint sea clutter from the sea waves, especially during anaprop, see Fig.5

Migrating birds give a special kind of clear air echos. Those birds appear in large enough quantities during nights of migration, in our climate spring and autumn, and give extensive weak echos centred around each radar, see Fig.5. Birds having regular habits, for instance leaving their roosting spots at the same time, are known to give radar echos (Vaugnh 1985) and radars have been used by ornithologists. The latter two cases, sea waves and birds, give Doppler velocities which are not representative for the wind.

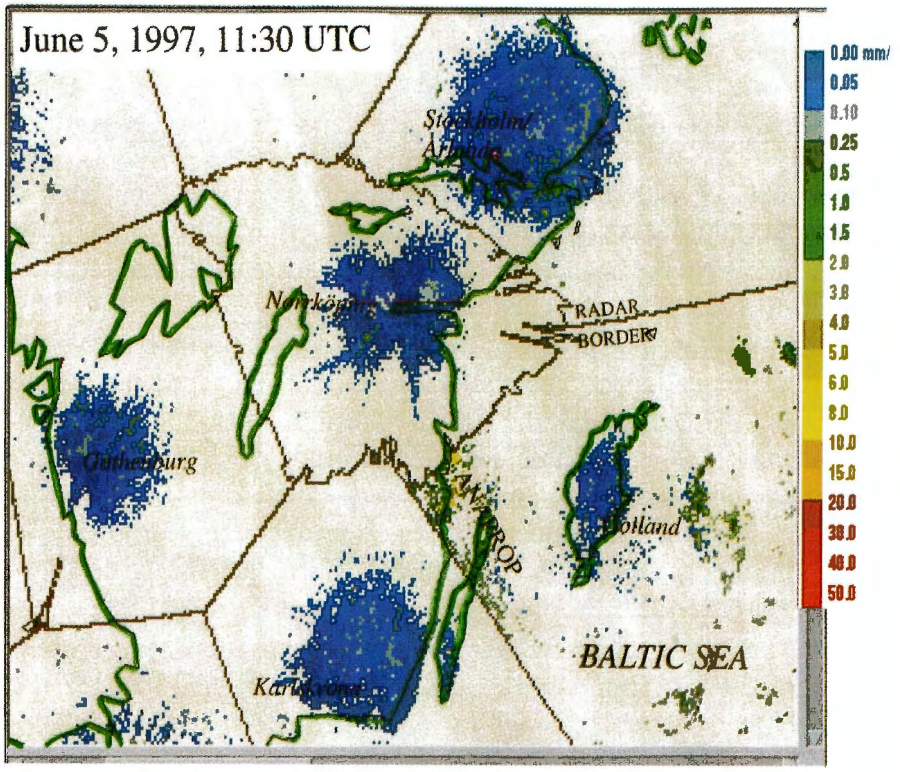

Fig. 1. Composite radar image, showing clear air echos from 5 radars an early summer day. Borders between the surveillance areas of the radars are shown by thick black lines, coasts by green lines. Over the Baltic Sea anomalous propagation gives echos from coasts and waves on the Gotland radar. NORDRAD, Non-Doppler mode, 5 June 1997 11:30 UTC.

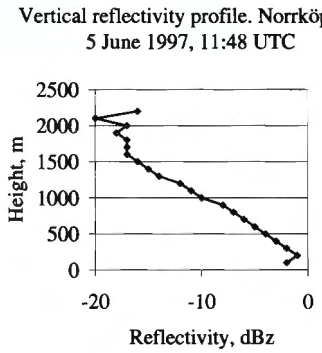

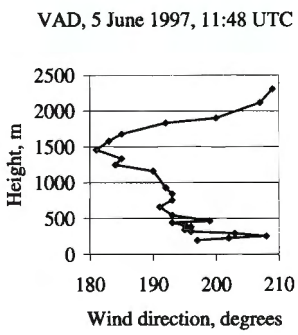

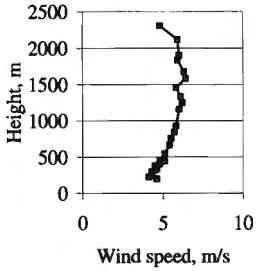

Fig. 2. Vertical profiles of reflectivity (above), wind direction and wind speed according to the VAD technique (right). The wind direction scale only spans 30°.
The Norrköping radar. Doppler mode, 5 June 1997, 11:48 UTC.

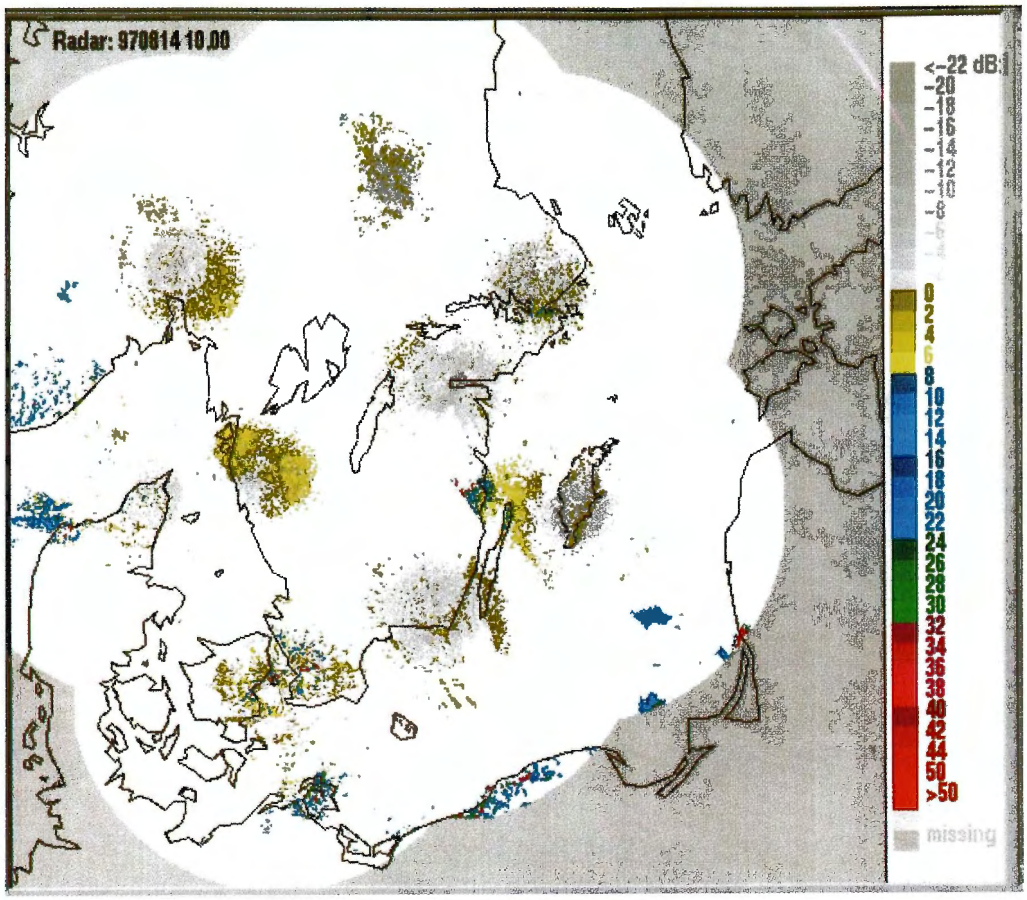

Fig. 3. Clear air echos a late summer day. Compared to Fig. 1 the echos reach somewhat more out into the sea. Also this day there was anaprop over the sea. Radars near a coast therefore may depict coasts and sea waves. NORDRAD, Non-Doppler mode, 14 Aug. 1997, 10:00 UTC

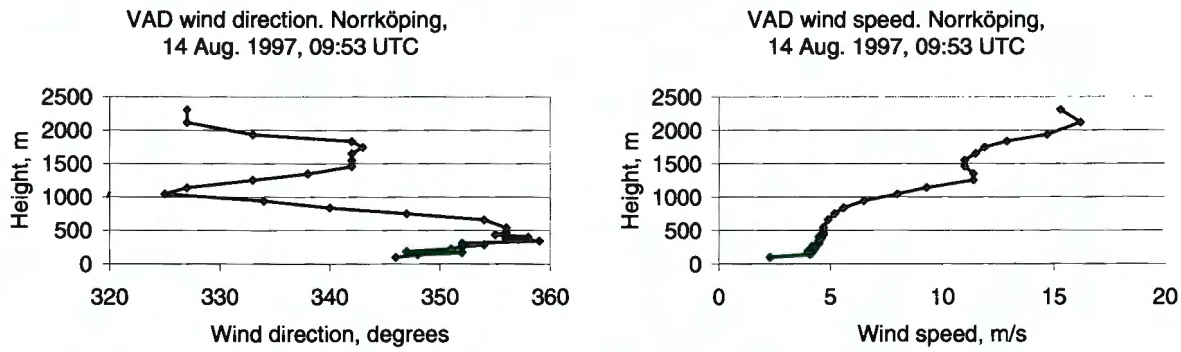

Fig. 4. VAD winds from clear air echos. The wind direction scale only spans 40°. Norrköping, 14 Aug. 1997, 09:53 UTC

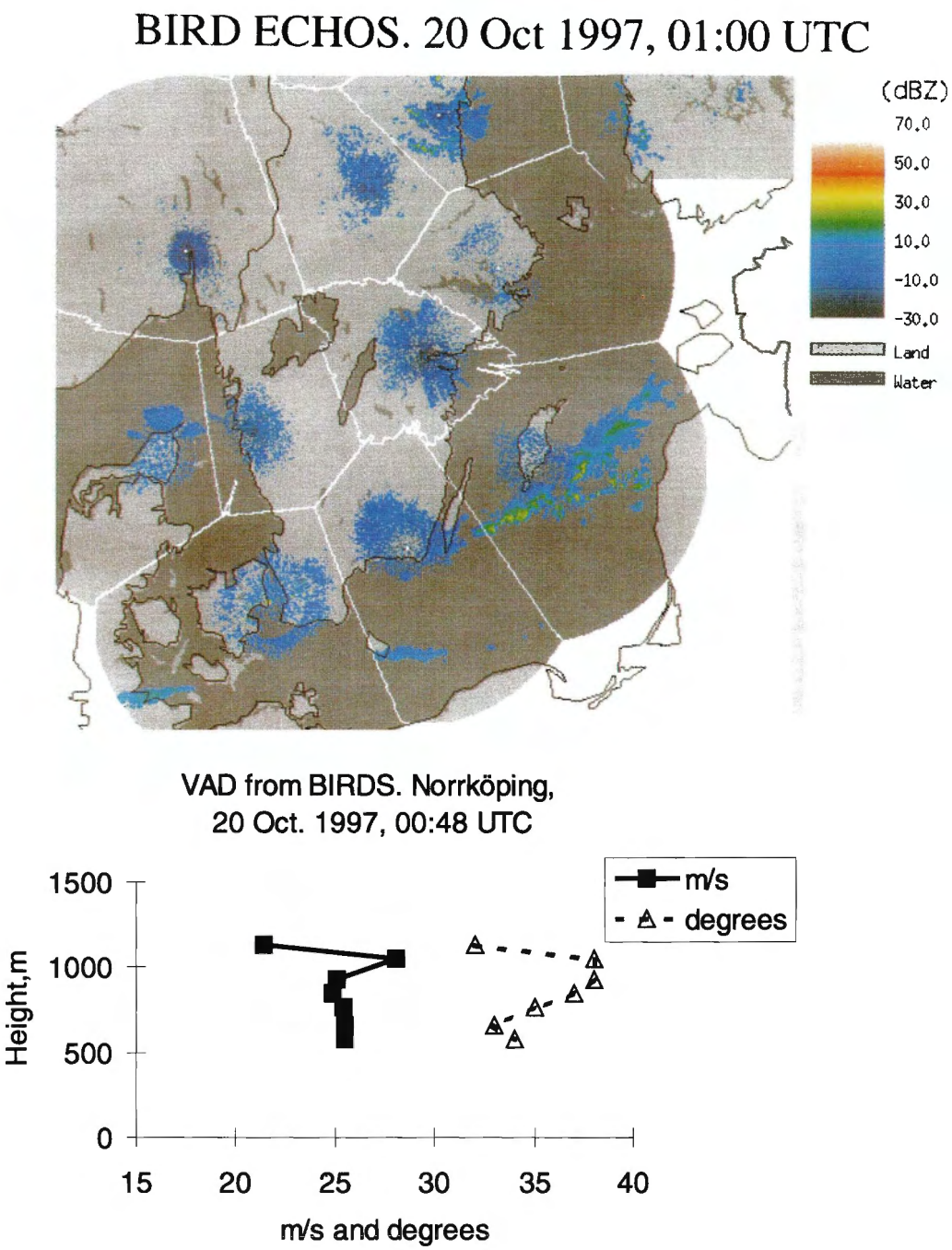

Fig. 5. Echos from migrating birds. The VAD 'winds' from the Norrköping radar are shown below the composite radar image. The radars of Sindal (northern tip of Denmark) and Hudiksvall (the northern-most radar) show also sea clutter. The wide-spread echo south and east of Gotland is precipitation from a cold front.
NORDRAD, non-Doppler mode, 20 Oct. 1997, 01:00 UTC.

4. Annual and daily march of clear air echos and their 3-D structure

In our climate clear air echos are common in the warmer seasons with an air temperature above about 8 °C. Generally they are most high-reaching and cover largest areas around the midday.

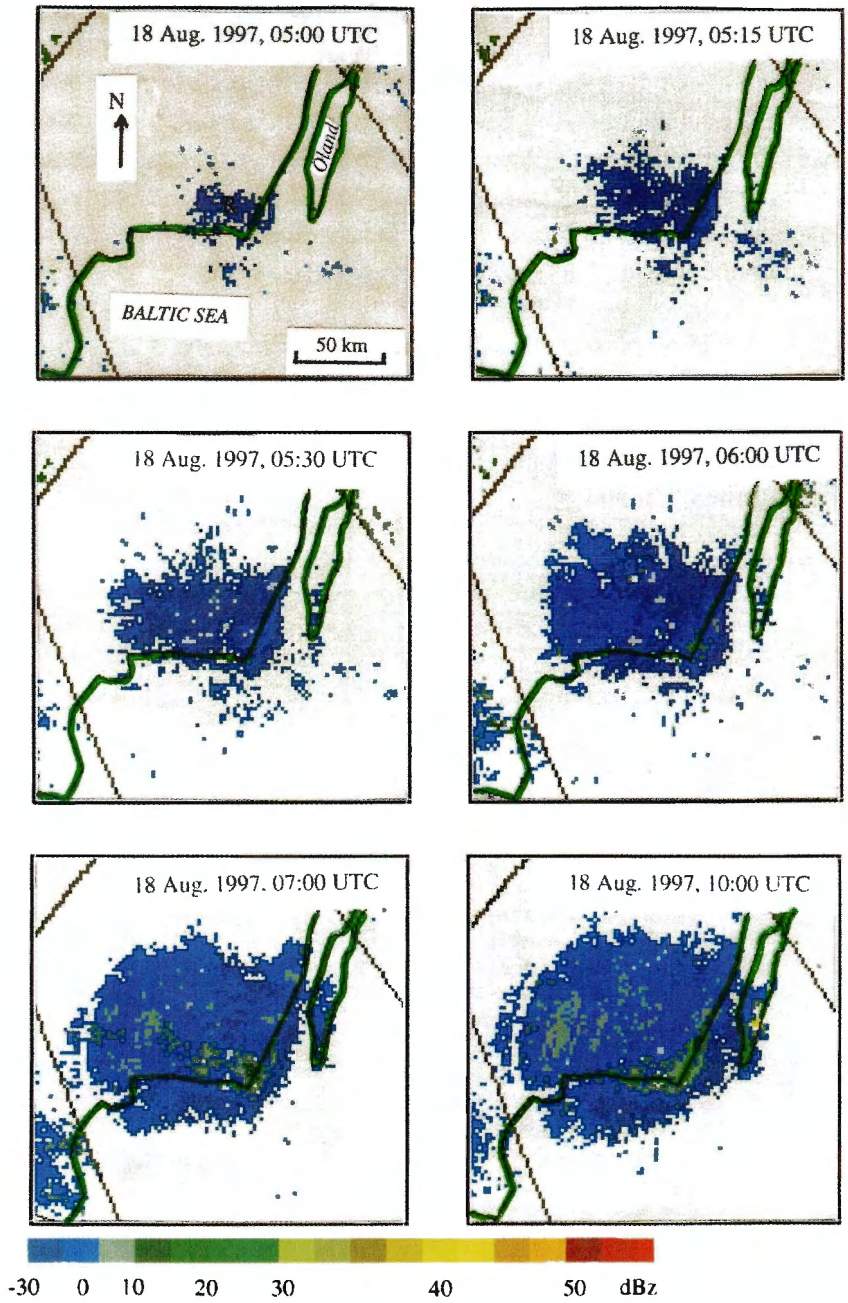

Fig. 6. Development of clear air echos shown by the Karlskrona radar. The growth is rapid between 05 and 06 UTC. After 05:30 UTC there is an echomaximum along the coast. Non-Doppler mode, 18 Aug. 1997.

Figs. 6, from the Karlskrona radar (56.30 ° N, 15.61 ° E), show the typical growth of clear air echos during the morning. The local time is 2 hours ahead of the UTC time. The sunrise was at 03:40 UTC. The weather was cloud-free, with weak northerly winds at anemometer level. About 1.5 hours after sunrise, at 05:00, the echos cover only a small, ellipsoid area around the radar. At the second time, 05:15 UTC, the echos have become somewhat asymmetric around the radar, since they have mainly increased their extent over land and do not extend so far out over the sea. Most of the strait between the mainland and the island of Öland is free from echos until 07:00 UTC, when the southern tip of the island is covered. At 08:00 UTC the echos have bridged the strait and at 10:00, that is local midday, they have reached their maximum horisontal extent. Their configuration is still asymmetric, the echos reaching farthest from the radar from

west to north, over land, where they have a radius of about 100 km. From 05:15 coastal maximums of echo strength indicate coastal convergence. In these maximums the reflectivities reach about 10 dBz, while generally the reflectivities are about or below 0 dBz. Such coastal maximums have been observed by Sauvageot and Despaux (1996), with a K_A (wavelength 0.86 cm) radar at the French Atlantic coast (Centre d'essais des Landes). At this wavelength clear air echos are due to particulate matter, as insects, and not to atmospheric dishomogenities giving Bragg scatter. During evenings bands of echos were transported from land to sea by the upper sea breeze.

The rapid clear air echo growth about two hours after sunrise is also shown by Fig. 7, giving the frequencies of echos at the CAPPI level of 500 m, according to the Norrköping radar. The area was a north-south oriented square, 80*80 km^2 , centred at the radar. The echos reach their maximum extent during forenoon, and taper of during the afternoon and the evening.

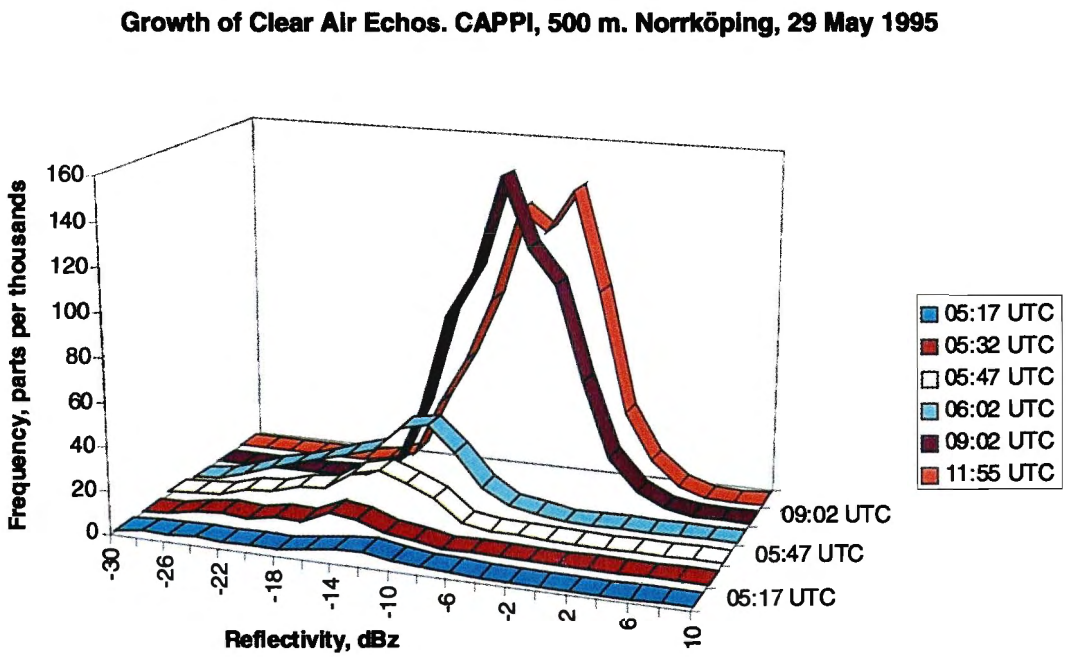

Fig. 7. Growth of clear air echos at CAPPI level 500 m. The area used is a north--south oriented square with a side of 80 km, centred at the antenna. Doppler mode, Norrköping, 29 May 1995, 05:17-11:55 UTC

The 3-dimensional clear air echo development during a cloudy day is shown by Fig. 8 a-c. There were 5-7 octas Stratocumulus, no precipitation and SW to W winds at anemometer level. At 08:47 UTC the echos reach about 1500 m, though there are only few about 600 m, in fact too few to permit wind estimates. The echos reach their maximum extent at about 1000 m, though the strongest echos appear at the lowest level. This may be due to contamination from ground echos. The wind speed increases much with height, indicating that the stratification of the atmosphere is fairly stable. One hour later, Fig. 8 b, the echos reach about 2000 m, and their maximum extent is still well above the surface, though the strongest echos still appear at the lowest height interval, and generally the echos are stronger. The VAD winds reach about 2000 m up,

and the speed still increases much with height, indicating a stable atmosphere. In the afternoon, Fig. 8 c, the 3-dimensional echo structure is very similar. The wind speed increase with height is weaker, indicating a less stable atmosphere.

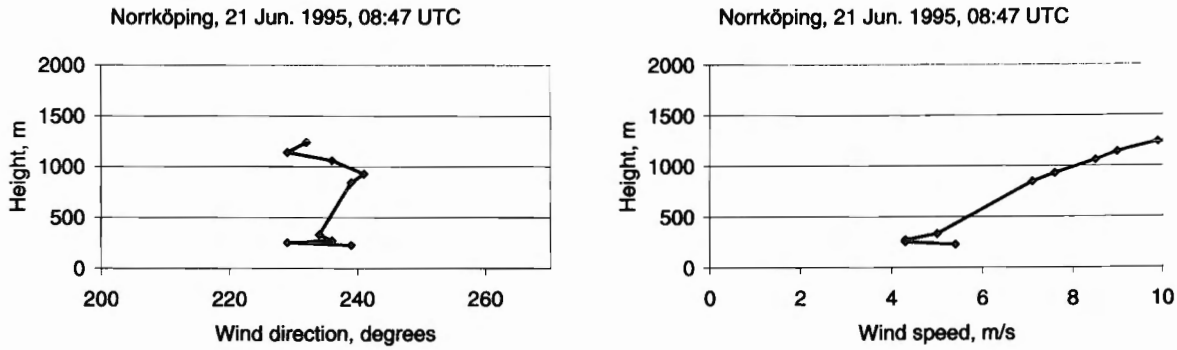

CLEAR AIR ECHOS. Norrköping, 21 June 1995, 08:47 UTC

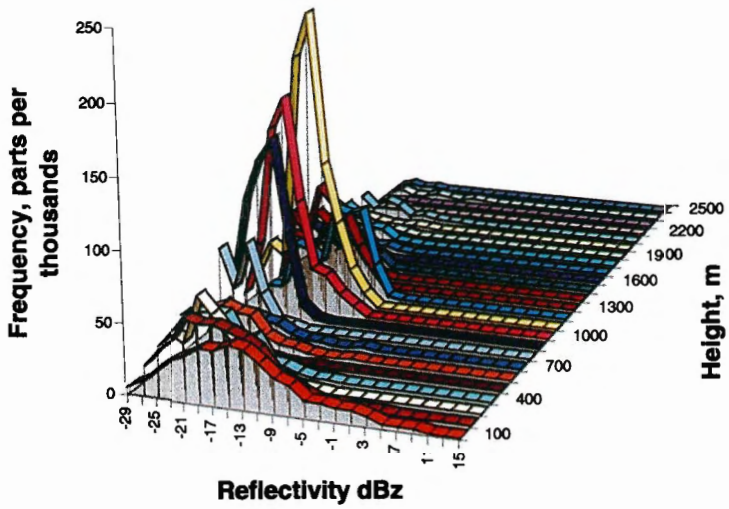

Fig. 8 a. VAD winds and distributions of reflectivity at different heights. At 08:47 UTC (10:47 local time) the echo maximum lies at about 1000 m height, the echos are relatively weak and the VAD records no winds between 360 and 810 m. The vertical wind speed gradient is large.

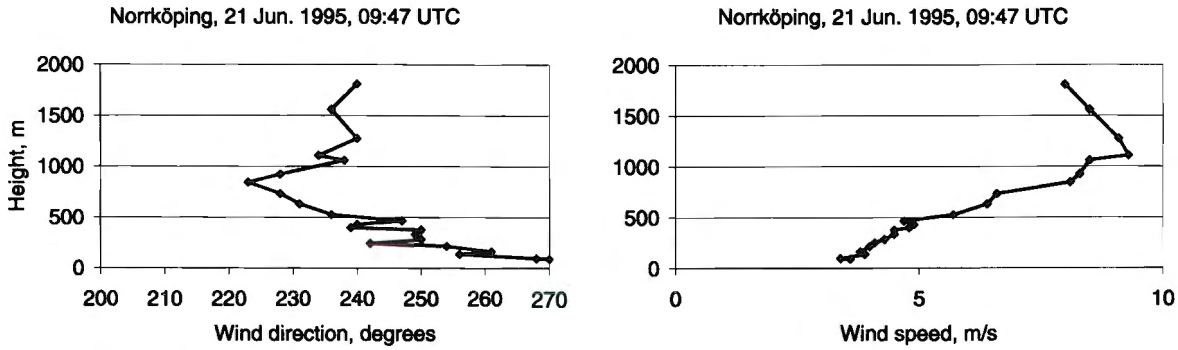

CLEAR AIR ECHOS. Norrköping, 21 June 1995, 09:47 UTC

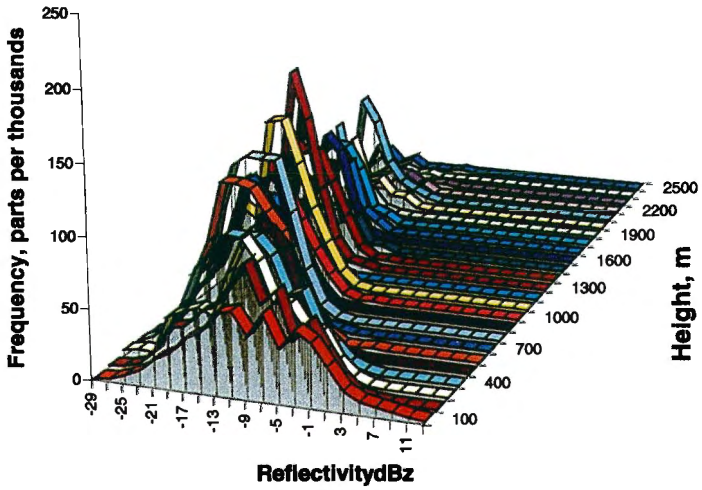

Fig. 8 b. VAD winds and distributions of reflectivity at different heights. At 09:47 UTC the VAD wind profile is unbroken up to its maximum height. There are more echos at the lowest levels, but still most echos just above 1000 m height.

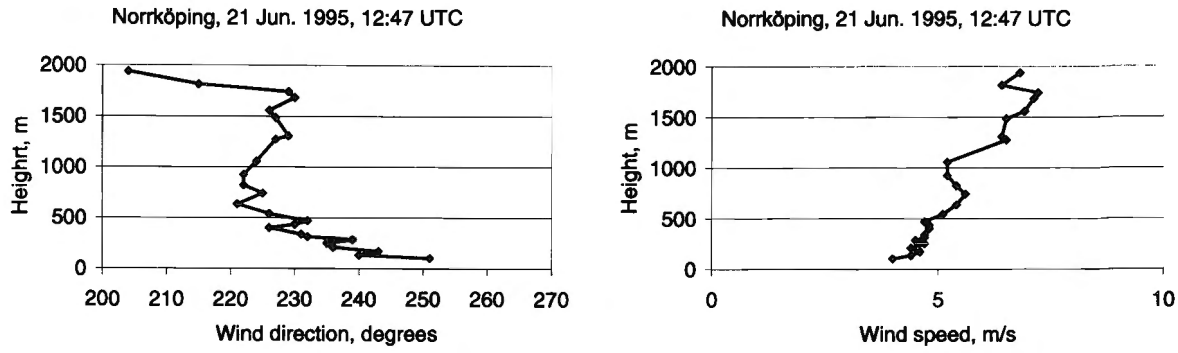

CLEAR AIR ECHOS. Norrköping, 21 June 1995, 12:47 UTC

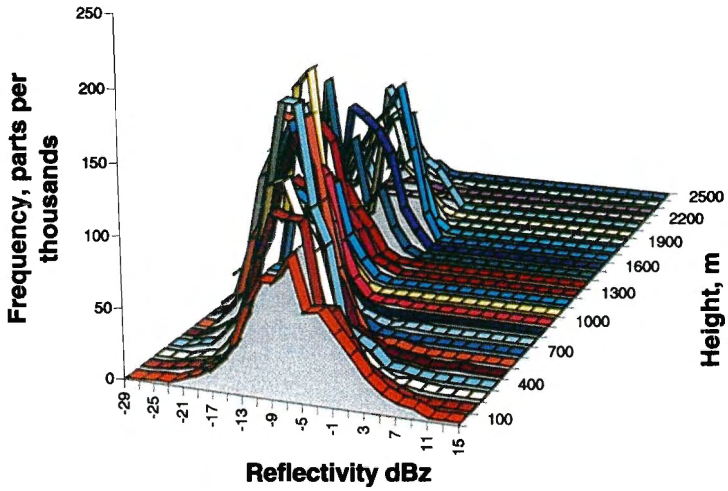

Fig. 8 c. VAD winds and distributions of reflectivity at different heights. At 12:47 UTC there are more echos above 1500 m, the VAD winds reach higher up and the vertical wind speed gradient is less.

The interplay between clear air echos, wind and temperature is exemplified by Fig. 9. The clear air echos appear in the planetary boundary layer. If there are enough clear air echos it is possible to reiterate the wind. Thus, the height to which winds are received gives a measure of the height of the boundary layer. This may be a somewhat too low estimate, since the VAD routine used requires echos in a fairly large area, but nevertheless must be considered a good estimate. Fig. 9 shows the rapid lifting of the boundary layer top, starting about two hours after sunrise and coinciding in time with the air temperature rise. As the turbulence grows, the wind at 300 m height is slowed. The boundary layer reaches its maximum height before the temperature maximum, and also tapers of before the temperature.

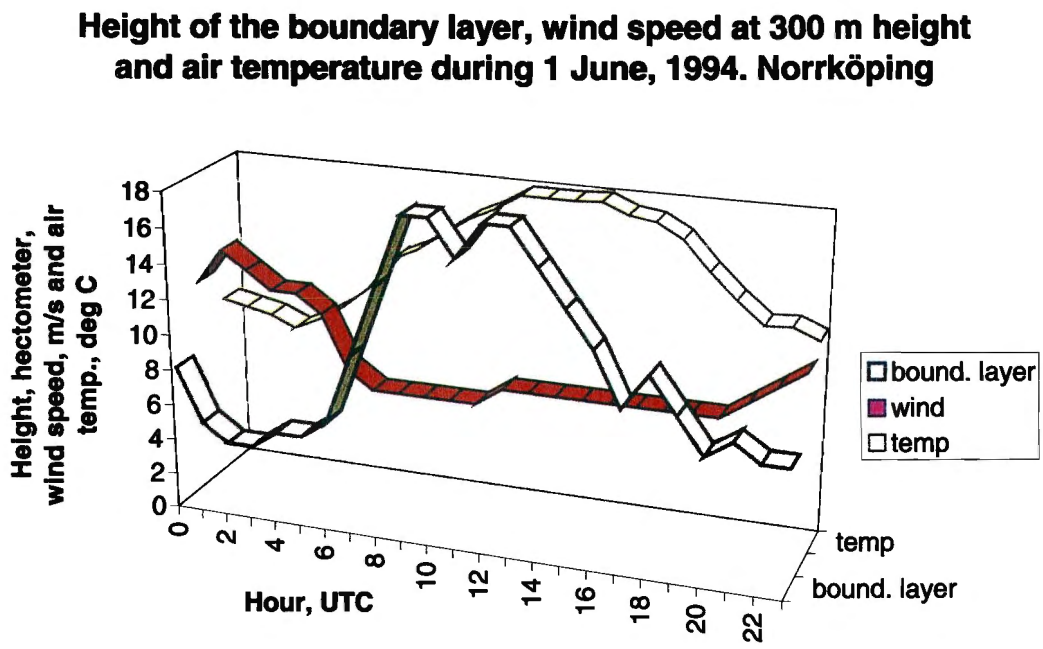

Fig. 9. Height of the boundary layer(=the height up to which VAD winds were obtained), VAD wind speed at 300 m height and air temperature at 2 m above the ground. Norrköping, 1 June 1994.

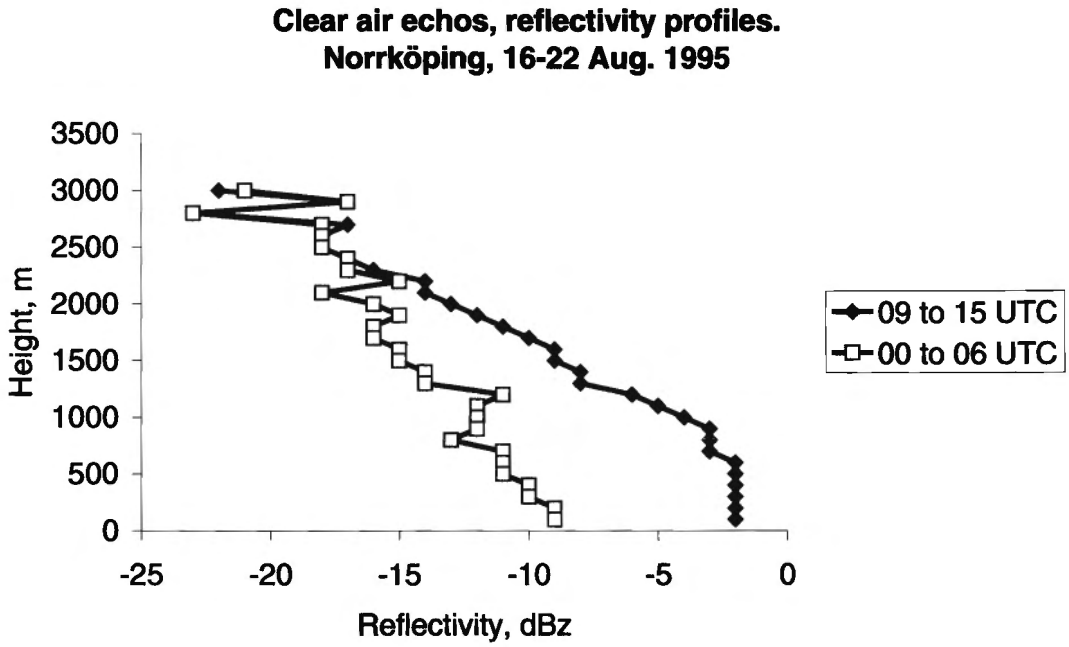

Fig. 10. Average vertical reflectivity profiles during a period with only clear air echos at late night (00-06 UTC) and day (09-15 UTC). Norrköping, 16-22 Aug. 1995.

5. A clear air echos event

16-22 Aug. 1995 the Norrköping radar only showed clear air echos, which were more abundant and stronger than usual. During daytime the echos usually extended to a radius of about 100 km from the antenna over land, but only a few km outside the coast. The coast east of Norrköping is about 50 km from the radar. The average reflectivity profiles during late night and the midday hours are shown by Fig. 10. The weak echos above 2 km have about the same strength at daytime and night, but below this height they are 5-10 dBz stronger during daytime. The frequency distributions of reflectivities at different heights are shown by Figs 11 a-b.

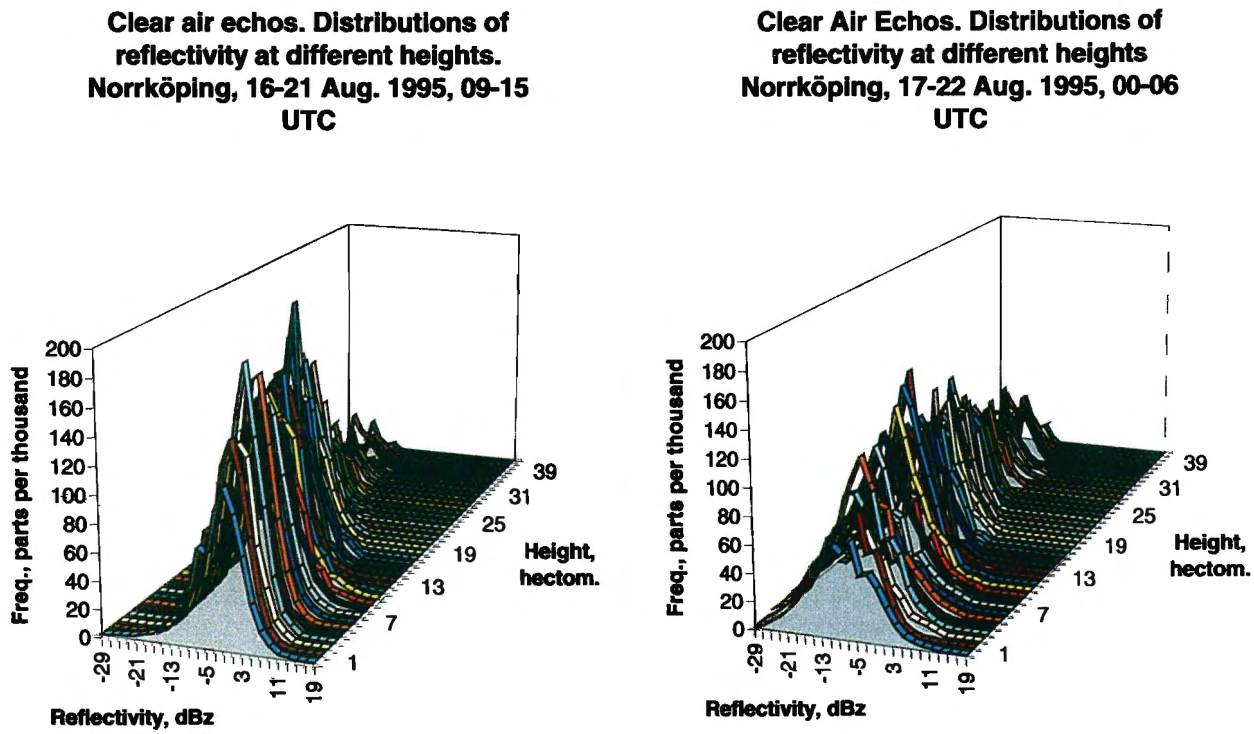

Fig 11 a,b. Frequency distributions of clear air echo reflectivities at different heights during day and night. Norrköping, 16-22 Aug 1995.

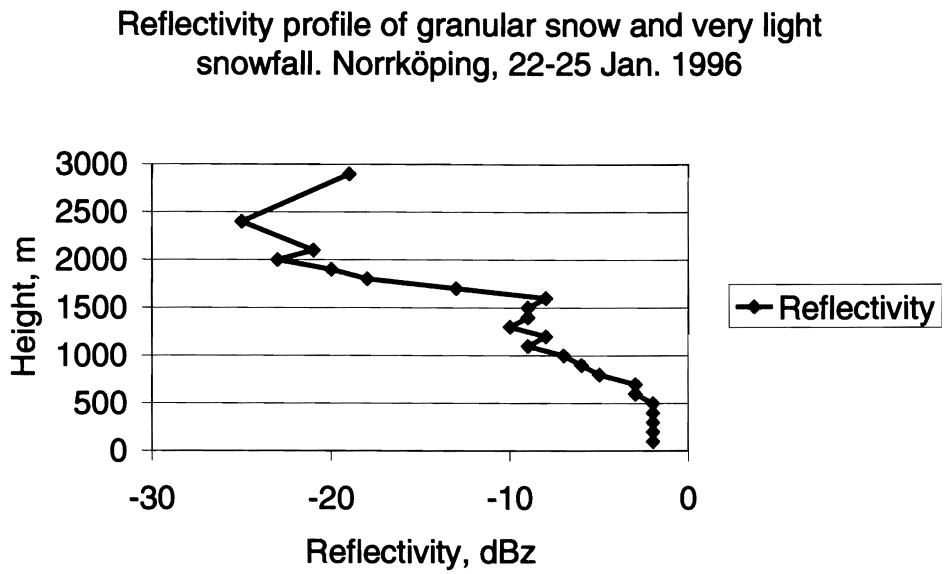

Fig. 12. Average reflectivity profile from winter precipitation in the form of granular snow and very light snowfall. Norrköping, 22-25 Jan. 1995.

It is interesting that the reflectivities and vertical extent of these clear air echos are similar to those from winter precipitation in the form of light and granular snow, Fig. 12, cf Fig. 10. The clear air echos are a summer phenomenon, but otherwise they are difficult or impossible to discern from faint precipitation echos in the reflectivity signature. Possibly the clear air echos are somewhat more patchy than faint precipitation echos. The Doppler wind information may be used for this task. Precipitation generally gives a smooth horisontal wind field, where most of the wind estimates are accepted by our VAD routine. Clear air echos give a more irregular wind field, and several wind estimates are rejected.

6. Frequency of clear air echos

From the preceding discussions it is evident that clear air echos are common during the warmer seasons, though precipitation monitoring is the main task for our weather radars. Fig. 13, for the summer month of June, shows a pronounced low-level maximum of faint radar echos at a height of 10 hectometers (1 km). This maximum is caused by clear air echos. At higher reflectivities the distribution is more irregular, with badly defined maxima between 5 and 25 dBz. These are due to rain. This Figure implies a bimodal distribution at this height, 1000 m, or 10 hectometers.

We can consider the echos to consist of two populations

- clear air echos
- precipitation echos.

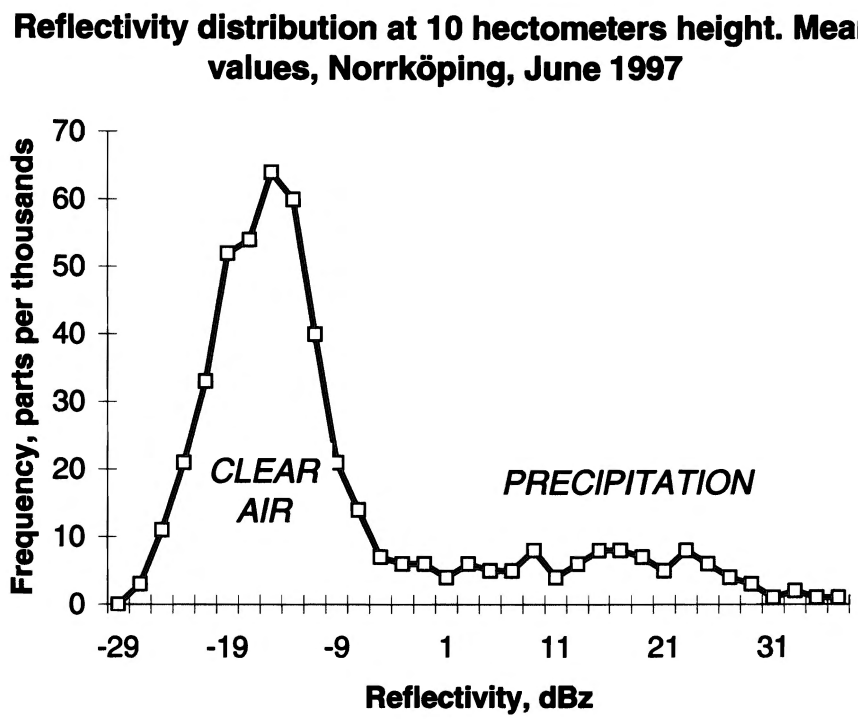

Fig. 13. The frequency distribution of reflectivities at 1000 m height suggests a bimodal distribution. The Norrköping radar, June 1997.

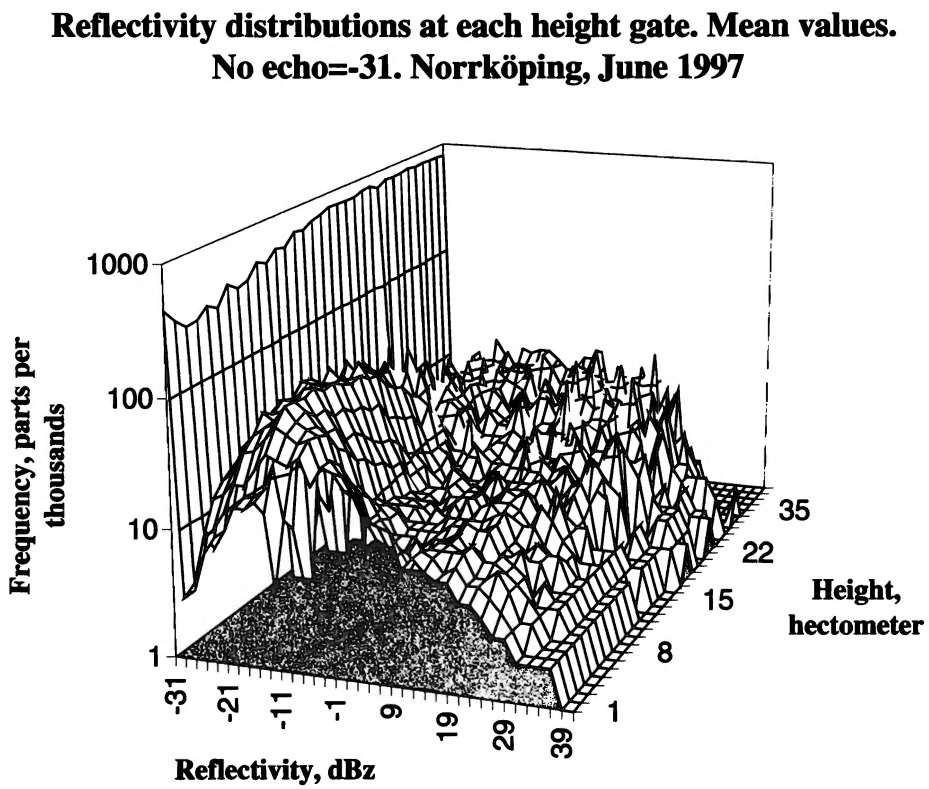

Fig. 14. 3-dimensional distribution of reflectivities during a summer month. This Figure also shows the non-echo frequencies (dBz=-31). Norrköping, June 1997.

At higher levels, Fig. 14, the low-level maximum disappears. In this Figure the frequency scale is logarithmic, in order discern the low frequencies of echos (about 10 parts per thousands) as well as the high frequencies (above 200 parts per thousands) of no echos (dBz=-31). The somewhat complicated Fig. 14 shows that
-at all levels the frequencies of no echos (dBz=-31) is dominant
- the low dBz frequency maximum (the clear air echos) disappears with height

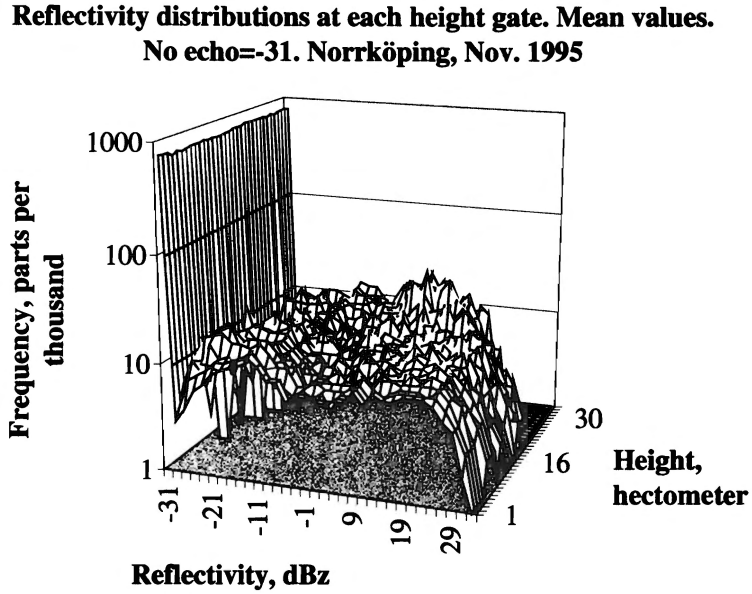

Fig. 15. 3-dimensional distribution of reflectivities during an autumn month. This Figure also shows the non-echo frequencies (dBz=-31). Norrköping, Nov. 1995.

Going to an autumn month, Nov., Fig. 15, we see that the echo frequencies are much lower, only about 10% or 100 parts per thousands. Still, however there are two frequency maxima at lower levels. The lowest one, at about -20 dBz is of unknown origin. It may be echos from clear air, but since these weak echos do not give any radial winds it may well be some technical artefact. The frequency maximum about 10 dBz is caused by precipitation, mainly in the form of snow.

In order to get a quantitative estimate of the occurrence of clear air echos we have used VAD soundings from the Göteborg radar (Andersson, 1998). Göteborg was selected because the radiosonde site, Landwetter lies only 10 km from the radar. Soundings for 00, 06, 12 and 18 hr UTC were classified into 'clear' and 'not clear' cases A data set from 9 Dec. 1994-14 Feb. 1995 and 28 Jun.-30 Nov. 1995 was available. Four cases with bird echos were removed. Unfortunately, the data does not cover the spring. All observations where a radiosounding was available were considered. The main pressure levels 925, 850, 700, 500 and 400 hPa were used.

At each level echos were considered present when the VAD gave an accepted wind estimate. This procedure should give somewhat too low clear air echo frequencies, and also too low heights, since there may be
- echos giving not accepted wind estimates
- echos, but too few to give a wind estimate.

The results are given in Table 3.

Table 3. Availability of VAD winds at Jonsered. The fraction (nr of soundings with wind)/(total number of soundings) is the availability. The whole period is 9 Dec. 1994 -1 Feb.1995 and 28 Jun.-30 Nov. 1995. Summer is 28 Jun.-30 Sep. 1995.

	PRESSURE LEVEL, hPa				
PERIOD AND WEATHER	*925*	*850*	*700*	*500*	*400*
Whole, Clear and not Clear, 00-24 UTC	*0.83*	*0.64*	*0.31*	*0.20*	*0.15*
Summer, not Clear, 00-24 UTC	*0.92*	*0.89*	*0.61*	*0.44*	*0.35*
Summer, Clear, 00-24 UTC	*0.94*	*0.76*	*0.15*		
Summer, Clear, 00 UTC	*0.98*	*0.72*	*0.13*		
Summer, Clear, 06 UTC	*0.83*	*0.59*	*0.16*		
Summer, Clear, 12 UTC	*0.94*	*0.98*	*0.30*		
Summer, Clear, 18 UTC	*1.00*	*0.74*	*0.06*		

It should be noticed that our study areas are close to the radar, for the reflectivity studies only within a radius of 15 km from the antenna. The radar is not able to detect these faint and relatively low targets at large ranges. Certainly these targets do not appear only close to our radars, but due to the beam broadening and curvature of the earth the radar is 'short-sighted' and the targets only appear as patches surrounding the radar, cf Figs 1, 3 and 5.

7. Echos from birds

As already discussed, Fig. 5, echos from migrating birds give nocturnal echos during spring and autumn. On a pseudo-CAPPI these echos are very similar to clear air echos. Generally, towards sunset the clear air echos diminish. During migration nights there is nearly an 'explosion' of faint echos after sunset and the echos may reach a radius of about 100 km. The echos prevail during night and disappear towards sunrise. Fig. 16 shows the distribution of reflectivities from a migration observation and the derived VAD 'winds'. In this case the birds had a strong tail wind. During migrations most of the VAD wind estimates fit so badly to the expected sine curve that they are rejected, but a few generally are good enough to give a wind estimate. In this respect they are similar to VAD winds from clear air echos; also then the numbers of rejected estimates are high, even if generally they are higher for birds. The bird echos may extend up to 2-3 km. Their reflectivities are generally well below 0 dBz, though some higher ones appear, as for instance 21 dBz at the lowest level in Fig.. 16. This could be a ground

echo. At higher levels there are some reflectivities of 7 dBz (these reflectivities originate from the non-Doppler mode and are not affected by the +5 dBz error that the non-Doppler mode had earlier). I have, however, not observed any bird echos above about 25 dBz, which is far from the strengths above 50 dBz that, according to Larkin (1991), large flocks of geese can give. Otherwise, the reflectivities generally are well below 0 dBz in accord with Larkins' results.

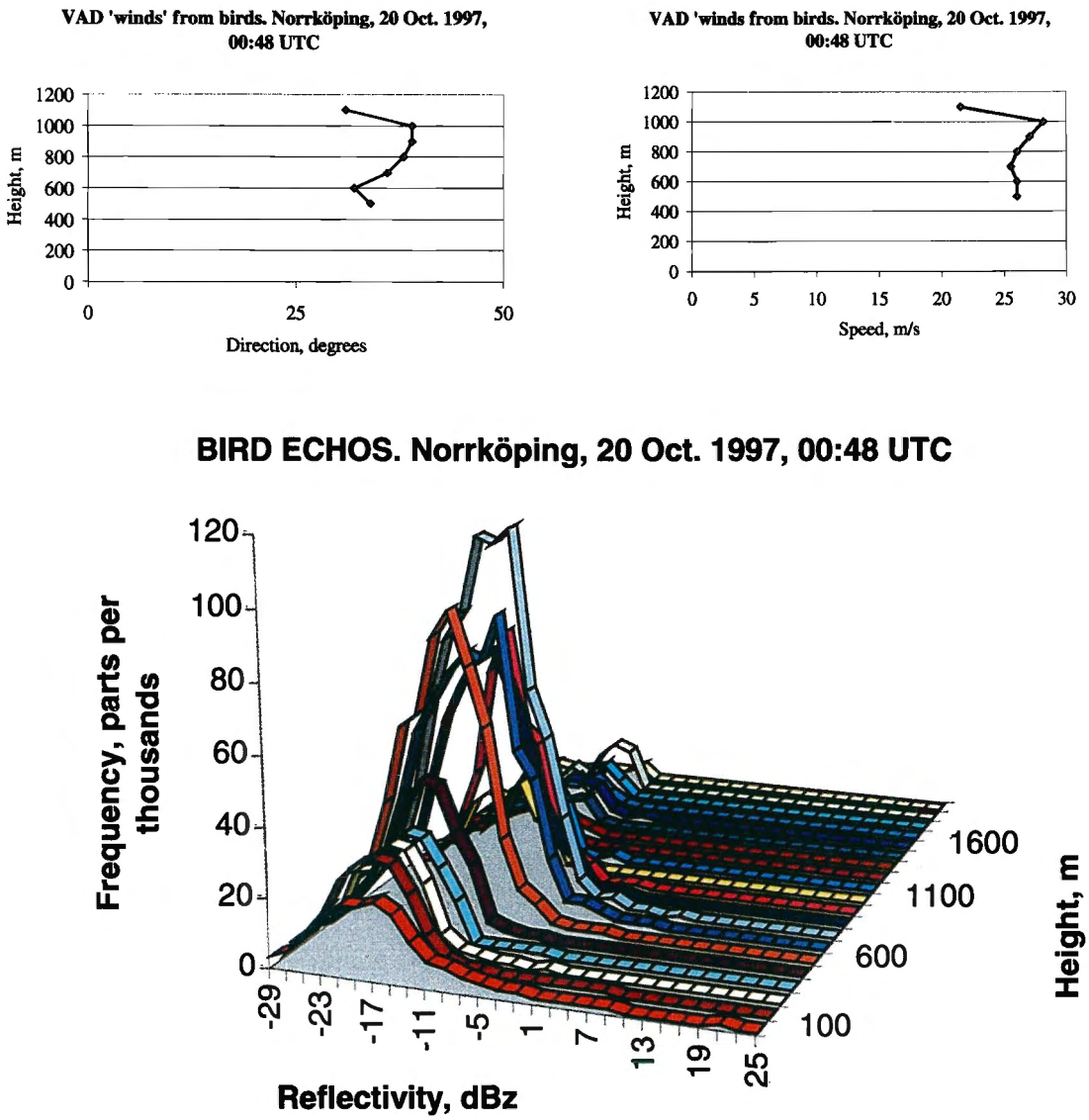

Fig. 16. 3-dimensional structure of echos from migrating birds and VAD 'winds' derived from them. The reflectivity structure of the echos from birds is very similar to that from clear air echos. Norrköping, Doppler mode, 20 Oct. 1997, 00:48 UTC.

Even if earlier analog weather radars, with their better time and range resolution, were more apt to bird observations, the weather radar of today offers many possibilities. In the US methods have been developed to use their radar system NEXRAD with the WSR-88D radar to monitor migrating birds (Gauthreaux and Belser 1998, Cunningham).

Prior to radar observations of migrating birds, there was an opinion among ornithologists that birds preferred to migrate in bad weather close to lows, often in headwind. This was due to biassed observations: radar studies show that birds prefer to migrate in good weather, choosing tailwind, but at so high altitudes that they cannot be seen from the ground (Koistinen, 2000). This illustrates the impact of weather radar in this field and also its potential for future work.

8. Echos from sea waves

Radars close to a coast may give echos from sea waves. This is especially true if the radar has a free horison towards the sea. During anomalous propagation such a radar may be contaminated by echos from waves out to a radius of about 200 km. These echos, though they often appear during clear air conditions, are not classified as clear air echos. The reason for mentioning them here is that wave echos are common on coast-near radars with a free horison and that they often appear during clear air conditions. Moreover, such echos may give VAD 'winds', which certainly are not representative for the atmospheric winds. Such VAD 'winds' are fairly common on the Gotland radar, where faint wave echos are common in one south-east and one south-west sector, Fig. 17. This sectors are centred at the directions giving the smallest distances to the coast. The originate from the lowest scan, elevation angle 0.5 °, and are probably due to the first side lobe, since they are caused by echos at a range of about 25 and have apparent heights of about 300 m. (A side lobe is a maximum of radiation outside the main lobe. The radiation intensity in the side lobes is <25 dB of the intensity of the main lobe).

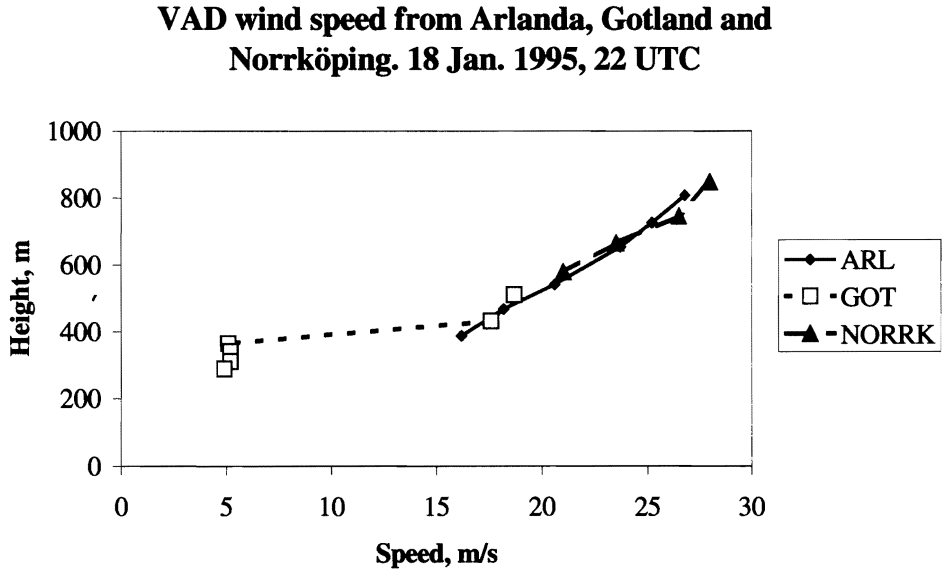

Fig. 17. Sea waves give VAD 'winds' at the lowest levels of the Gotland radar. The wind field was uniform and above the 'wave speeds' the soundings agree. At Gotland the wind speed at anemometer level was about 10 m/s. 18 Jan. 1995, 22 UTC

9. Discussion and conclusions

During the warmer seasons our C band Doppler weather radars nearly always detect echos from a non-precipitating atmosphere, that is clear air echos. Such echos are rare during winter, though they may appear also then. The winter clear air echos have much smaller horisontal as well as vertical extent than the summer ones. Horisontally the latter may reach a radius of about 100 km from the antenna, and vertically up to about 3 km above the ground. The summer clear air echos have a diurnal variation characterised by minimum extent as well as reflectivity just after sunrise and maximal values of these parameters about local midday.

The source of these echos may be sharp gradients of the refractive index of the air, or insects. Since theoretical calculations show that it is difficult to get the sharp refractive index gradients required, insects are the most probable cause. In fact, entomologists have since long ago used radars, with frequencies close to the C band, for insect studies. Since both these targets by and large follow the wind they can be utilised for wind measurements (Andersson, 1998). However, migrating birds are targets that do not follow the winds. Generally such birds have fairly regular habits, permitting identification. The migrating birds of our region appear mainly during spring and autumn nights, flying towards north during spring and towards south during autumn. The weather radar of today has a great potential also in ornithology as well as entomology.

Acknowledgements: This work was supported by the European Commission, project *Development of advanced Radar Technology for Application to Hydrometeorology (DARTH)*, contract ENV4-CT96-0262.

References:

Achtemeier, G.L., 1991: The use of insects as tracers for "Clear-Air" boundary layer studies by Doppler radar. *J. Atmos. Oceanic Technol.,* **8**, 746-765.

Andersson, T., 1992: A method for estimating the wind profile and vertical speed of targets from a single Doppler radar. *Instruments and Observing Methods,* Report No. 49, WMO/TD, No. 462, p. 380-386.

Andersson, T., 1998: VAD winds from C band Ericsson Doppler weather radars. *Meteorologische Zeitschrift,* N.F. **7**, 309-319.

Cunningham, A. : http://virtual.clemson.edu.groups/birdrad/comment.htm

Engelbart D. and U. Görsdorf, 1997: Effects and observations of migrating birds on a boundary-layer windprofiler in eastern Germany. *Extended Abstracts, COST-76 Profiler Workshop 1997,* Engelberg, Switzerland, 227-229.

Gauthreaux, S. A. Jr. and C. G. Belser, 1998: Displays of Bird Movements on the WSR-88D: Patterns and Quantification. *Weather and Forecasting,* **13**, 453-464.

Koistinen, J., 2000: Bird Migration Patterns on Weather Radar. *Phys. Chem. Earth (B),* **25**, 1185-1193.

Larkin, R. P., 1991: Sensitivity of NEXRAD algorithms to echoes from birds and insects. *Preprints, 25th Int. Conf. Radar Meteor.,* Paris, France, 203-206.

O'Bannon, T., 1995: Anomalous WSR-88D wind profiles - migrating birds? *Preprints, 27th Conf. Radar Meteor.,* Vail, Colorado, 663-665.

Pratte, J. F. and R. J. Keeler, 1986: Sensitivities of operational weather radars. *Preprints, 27th Conf. Radar Meteor.,* Snowmass, Colorado, JP 333-336.

Sauvageot H. and G. Despaux, 1996: The Clear-Air Coastal Vespertine Radar Bands. *Bull. Amer. Meteor. Soc.,* **77**, 673-681.

Vaughn, C., 1985: Birds and Insects as Radar Targets. A Review. *Proc. IEEE,* **73**, 205-227.

Wilson, J.W., T.M. Weckwerth, J. Vivekanandan, R.M. Wakimoto and R.W. Russell, 1994: Boundary Layer Clear-Air Radar Echoes: Origin of Echoes and Accuracy of Derived Winds. *J. Atm. Ocean. Techn.,* **11**, 1184-1206.

APPENDIX

Technical data for the Ericsson Doppler weather radar

Antenna	
Diameter	4.2 m
Gain	44.9 dB
Beam Width	0.9°
Polarization	Linear horizontal
Radome	
Diameter	6.7 m
Transmission loss	<0.2 dB
Antenna servo	
Azimuth movement	360° up to 6 rpm
Azimuth accuracy	0.2°
Elevation movement	-1° to 90°
Elevation accuracy	0.1°
Transmitter	
Frequency	5600 – 5650 MHz
Output power	250 kW
Pulse width	0.5 μs and 2.0 μs
PRF	250 Hz and 900/1200 Hz
Receiver	
Sensitivity	Better than –109 dBm (non-Doppler). Better than –114 dBm (Doppler)
Dynamic range	>85 dB (log receiver), > 87 dB (linear receiver with IAGC)
Signal processor	
A/D conversion	8 bits
Sampling rate	333 m nominally (non-Doppler), 83 m (Doppler)
Range integration	6 samples(non-Doppler), 12 samples (Doppler)
Instrumented range	480 km (non-Doppler), 120 km (Doppler)
Range resolution	2 km (non-Doppler), 1 km (Doppler)
Azimuth integration	1-64 pulses (non-Doppler), 2*32 pulses FFT (Doppler)
Data outputs	Reflectivity, radial velocity (Doppler only), spectrum width (Doppler only)
Data corrections	Range dependence, atmospheric attenuation and rain attenuation
Data resolution	Reflectivity 0.4 dBz, velocity 0.375 m/s, spectrum width 2 m/s classes
Data coverage	Reflectivity -30 to +72 dBz, velocity –48 to +48 m/s, spectrum width 4 classes: 0-2, 2-4, 4-6 and >6 m/s
Data accuracy	Reflectivity 1 dB Velocity <0.3 m/s 10 dB S/N, <0.6 m/s 0 dB S/N

SMHIs publications

SMHI publishes six report series. Three of these, the R-series, are intended for international readers and are in most cases written in English. For the others the Swedish language is used.

Names of the Series	**Published since**
RMK (Report Meteorology and Climatology)	1974
RH (Report Hydrology)	1990
RO (Report Oceanography)	1986
METEOROLOGI	1985
HYDROLOGI	1985
OCEANOGRAFI	1985

Earlier issues published in serie RMK

1 Thompson, T., Udin, I., and Omstedt, A. (1974)
Sea surface temperatures in waters surrounding Sweden.

2 Bodin, S. (1974)
Development on an unsteady atmospheric boundary layer model.

3 Moen, L. (1975)
A multi-level quasi-geostrophic model for short range weather predictions.

4 Holmström, I. (1976)
Optimization of atmospheric models.

5 Collins, W.G. (1976)
A parameterization model for calculation of vertical fluxes of momentum due to terrain induced gravity waves.

6 Nyberg, A. (1976)
On transport of sulphur over the North Atlantic.

7 Lundqvist, J.-E., and Udin, I. (1977)
Ice accretion on ships with special emphasis on Baltic conditions.

8 Eriksson, B. (1977)
Den dagliga och årliga variationen av temperatur, fuktighet och vindhastighet vid några orter i Sverige.

9 Holmström, I., and Stokes, J. (1978)
Statistical forecasting of sea level changes in the Baltic.

10 Omstedt, A., and Sahlberg, J. (1978)
Some results from a joint Swedish-Finnish sea ice experiment, March, 1977.

11 Haag, T. (1978)
Byggnadsindustrins väderberoende, seminarieuppsats i företagsekonomi, B-nivå.

12 Eriksson, B. (1978)
Vegetationsperioden i Sverige beräknad från temperaturobservationer.

13 Bodin, S. (1979)
En numerisk prognosmodell för det atmosfäriska gränsskiktet, grundad på den turbulenta energiekvationen.

14 Eriksson, B. (1979)
Temperaturfluktuationer under senaste 100 åren.

15 Udin, I., och Mattisson, I. (1979)
Havsis- och snöinformation ur datorbearbetade satellitdata - en modellstudie.

16 Eriksson, B. (1979)
Statistisk analys av nederbördsdata. Del I. Arealnederbörd.

17 Eriksson, B. (1980)
Statistisk analys av nederbördsdata. Del II. Frekvensanalys av månadsnederbörd.

18 Eriksson, B. (1980)
Årsmedelvärden (1931-60) av nederbörd, avdunstning och avrinning.

19 Omstedt, A. (1980)
A sensitivity analysis of steady, free floating ice.

20 Persson, C., och Omstedt, G. (1980)
En modell för beräkning av luftföroreningars spridning och deposition på mesoskala.

21 Jansson, D. (1980)
Studier av temperaturinversioner och vertikal vindskjuvning vid Sundsvall-Härnösands flygplats.

22 Sahlberg, J., and Törnevik, H. (1980)
A study of large scale cooling in the Bay of Bothnia.

23 Ericson, K., and Hårsmar, P.-O. (1980)
Boundary layer measurements at Klock-rike. Oct. 1977.

24 Bringfelt, B. (1980)
A comparison of forest evapotranspiration determined by some independent methods.

25 Bodin, S., and Fredriksson, U. (1980)
Uncertainty in wind forecasting for wind power networks.

26 Eriksson, B. (1980)
Graddagsstatistik för Sverige.

27 Eriksson, B.(1981)
Statistisk analys av nederbördsdata. Del III. 200-åriga nederbördsserier.

28 Eriksson, B. (1981)
Den "potentiella" evapotranspirationen i Sverige.

29 Pershagen, H. (1981)
Maximisnödjup i Sverige (perioden 1905-70).

30 Lönnqvist, O. (1981)
Nederbördsstatistik med praktiska tillämpningar.
(Precipitation statistics with practical applications.)

31 Melgarejo, J.W. (1981)
Similarity theory and resistance laws for the atmospheric boundary layer.

32 Liljas, E. (1981)
Analys av moln och nederbörd genom automatisk klassning av AVHRR-data.

33 Ericson, K. (1982)
Atmospheric boundary layer field experiment in Sweden 1980, GOTEX II, part I.

34 Schoeffler, P. (1982)
Dissipation, dispersion and stability of numerical schemes for advection and diffusion.

35 Undén, P. (1982)
The Swedish Limited Area Model. Part A. Formulation.

36 Bringfelt, B. (1982)
A forest evapotranspiration model using synoptic data.

37 Omstedt, G. (1982)
Spridning av luftförorening från skorsten i konvektiva gränsskikt.

38 Törnevik, H. (1982)
An aerobiological model for operational forecasts of pollen concentration in the air.

39 Eriksson, B. (1982)
Data rörande Sveriges temperaturklimat.

40 Omstedt, G. (1984)
An operational air pollution model using routine meteorological data.

41 Persson, C., and Funkquist, L. (1984)
Local scale plume model for nitrogen oxides. Model description.

42 Gollvik, S. (1984)
Estimation of orographic precipitation by dynamical interpretation of synoptic model data.

43 Lönnqvist, O. (1984)
Congression - A fast regression technique with a great number of functions of all predictors.

44 Laurin, S. (1984)
Population exposure to SO and NO_x from different sources in Stockholm.

45 Svensson, J. (1985)
Remote sensing of atmospheric tempera-ture profiles by TIROS Operational Vertical Sounder.

46 Eriksson, B. (1986)
Nederbörds- och humiditetsklimat i Sverige under vegetationsperioden.

47 Taesler, R. (1986)
Köldperioden av olika längd och förekomst.

48 Wu Zengmao (1986)
Numerical study of lake-land breeze over Lake Vättern, Sweden.

49 Wu Zengmao (1986)
Numerical analysis of initialization procedure in a two-dimensional lake breeze model.

50 Persson, C. (1986)
Local scale plume model for nitrogen oxides. Verification.

51 Melgarejo, J.W. (1986)
An analytical model of the boundary layer above sloping terrain with an application to observations in Antarctica.

52 Bringfelt, B. (1986)
Test of a forest evapotranspiration model.

53 Josefsson, W. (1986)
Solar ultraviolet radiation in Sweden.

54 Dahlström, B. (1986)
Determination of areal precipitation for the Baltic Sea.

55 Persson, C. (SMHI), Rodhe, H. (MISU), De Geer, L.-E. (FOA) (1986)
The Chernobyl accident - A meteorological analysis of how radionucleides reached Sweden.

56 Persson, C., Robertson, L. (SMHI), Grennfelt, P., Kindbom, K., Lövblad, G., och Svanberg, P.-A. (IVL) (1987)
Luftföroreningsepisoden över södra Sverige 2 - 4 februari 1987.

57 Omstedt, G. (1988)
An operational air pollution model.

58 Alexandersson, H., Eriksson, B. (1989)
Climate fluctuations in Sweden 1860 - 1987.

59 Eriksson, B. (1989)
Snödjupsförhållanden i Sverige - Säsongerna 1950/51 - 1979/80.

60 Omstedt, G., Szegö, J. (1990)
Människors exponering för luftföroreningar.

61 Mueller, L., Robertson, L., Andersson, E., Gustafsson, N. (1990)
Meso-γ scale objective analysis of near surface temperature, humidity and wind, and its application in air pollution modelling.

62 Andersson, T., Mattisson, I. (1991)
A field test of thermometer screens.

63 Alexandersson, H., Gollvik, S., Meuller, L. (1991)
An energy balance model for prediction of surface temperatures.

64 Alexandersson, H., Dahlström, B. (1992)
Future climate in the Nordic region - survey and synthesis for the next century.

65 Persson, C., Langner, J., Robertson, L. (1994)
Regional spridningsmodell för Göteborgs och Bohus, Hallands och Älvsborgs län. (A mesoscale air pollution dispersion model for the Swedish west-coast region. In Swedish with captions also in English.)

66 Karlsson, K.-G. (1994)
Satellite-estimated cloudiness from NOAA AVHRR data in the Nordic area during 1993.

67 Karlsson, K-G. (1996)
Cloud classifications with the SCANDIA model.

68 Persson, C., Ullerstig, A. (1996)
Model calculations of dispersion of lindane over Europe. Pilot study with comparisons to measurements around the Baltic Sea and the Kattegat.

69 Langner, J., Persson, C., Robertson, L., and Ullerstig, A. (1996)
Air pollution Assessment Study Using the MATCH Modelling System. Application to sulfur and nitrogen compounds over Sweden 1994.

70 Robertson, L., Langner, J., Engardt, M. (1996)
MATCH - Meso-scale Atmosperic Transport and Chemistry modelling system.

71 Josefsson, W. (1996)
Five years of solar UV-radiation monitoring in Sweden.

72 Persson, C., Ullerstig, A., Robertson, L., Kindbom, K., Sjöberg, K. (1996)
The Swedish Precipitation Chemistry Network. Studies in network design using the MATCH modelling system and statistical methods.

73 Robertson, L. (1996)
Modelling of anthropogenic sulfur deposition to the African and South American continents.

74 Josefsson, W. (1996)
Solar UV-radiation monitoring 1996.

75 Häggmark, L., Ivarsson, K.-I. (SMHI), Olofsson, P.-O. (Militära vädertjänsten). (1997)
MESAN - Mesoskalig analys.

76 Bringfelt, B, Backström, H, Kindell, S, Omstedt, G, Persson, C, Ullerstig, A. (1997)
Calculations of PM-10 concentrations in Swedish cities- Modelling of inhalable particles

77 Gollvik, S. (1997)
The Teleflood project, estimation of precipitation over drainage basins.

78 Persson, C., Ullerstig, A. (1997)
Regional luftmiljöanalys för Västmanlands län baserad på MATCH modell-beräkningar och mätdata - Analys av 1994 års data

79 Josefsson, W., Karlsson, J.-E. (1997)
Measurements of total ozone 1994-1996.

80 Rummukainen, M. (1997)
Methods for statistical downscaling of GCM simulations.

81 Persson, T. (1997)
Solar irradiance modelling using satellite retrieved cloudiness - A pilot study

82 Langner, J., Bergström, R. (SMHI) and Pleijel, K. (IVL) (1998)
European scale modelling of sulfur, oxidized nitrogen and photochemical oxidants. Model development and evaluation for the 1994 growing season.

83 Rummukainen, M., Räisänen, J., Ullerstig, A., Bringfelt, B., Hansson, U., Graham, P., Willén, U. (1998)
RCA - Rossby Centre regional Atmospheric climate model: model description and results from the first multi-year simulation.

84 Räisänen, J., Döscher, R. (1998)
Simulation of present-day climate in Northen Europé in the HadCM2 OAGCM.

85 Räisänen, J., Rummukainen, M., Ullerstig, A., Bringfelt, B., Ulf Hansson, U., Willén, U. (1999)
The First Rossby Centre Regional Climate Scenario - Dynamical Downscaling of CO_2-induced Climate Change in the HadCM2 GCM.

86 Rummukainen, Markku. (1999)
On the Climate Change debate

87 Räisänen, Jouni (2000)
CO_2-induced climate change in northern Europé: comparison of 12 CMIP2 experiments.

88 Engardt, Magnuz (2000)
Sulphur simulations for East Asia using the MATCH model with meteorological data from ECMWF.

89 Persson, Thomas (2000)
Measurements of Solar Radiation in Sweden 1983-1998

90 Daniel B. Michelson, Tage Andersson
Swedish Meteorological and Hydrological Institute (2000)
Jarmo Koistinen, Finnish Meteorological Institute
Christopher G. Collier, Telford Institute of Environmental Systems, University of Salford
Johann Riedl, German Weather Service
Jan Szturc, Instiute of Meteorology and Water Management
Uta Gjertsen, The Norwegian Meteorological Institute
Aage Nielsen, Danish Meteorological Institute
Søren Overgaard, Danish Meteorological Institute
BALTEX Radar Data Centre Products and their Methodologies

91 Josefsson, Weine (2000)
Measurements of total ozone 1997 – 1999

SMHI
Swedish Meteorological and Hydrological Institute
SE 601 76 Norrköping, Sweden.
Tel +46 11-495 80 00. Fax +46 11-495 80 01

ISSN 0347-2116